Systematic comparison of positron- and electron-impact excitation of the ν_3 vibrational mode of CF_4

J. P. Marler and C. M. Surko
Department of Physics, University of California, San Diego, 9500 Gilman Drive, La Jolla, California 92093-0319, USA
(Received 13 August 2005; published 8 December 2005)

Absolute measurements are presented for the excitation of the ν_3 vibrational mode in CF_4 by positron and electron impact from 0.1 to 2 eV. To minimize systematic differences, these measurements were made using the same trap-based electron or positron beam, associated experimental apparatus, and procedures. Unlike other vibrational excitation cross sections studied to date, the near-threshold cross section for the ν_3 vibrational mode in CF_4 is similar, both in magnitude and shape, for positrons and electrons. Comparison of the cross sections with an analytic Born dipole model yields good agreement, while comparison of this model with other measured positron-impact vibrational cross sections indicates that the contribution of this long-range dipole coupling varies widely. The maximum value of the cross section in CF_4 is the largest of any positron-impact vibrational excitation cross section measured to date. This provides a likely explanation of the observation that CF_4 is very effective when used as a buffer gas to cool positron gases and plasmas.

DOI: 10.1103/PhysRevA.72.062702 PACS number(s): 34.85.+x, 34.50.Ez

I. INTRODUCTION

Understanding vibrational excitation processes is important for numerous applications involving both positrons and electrons [1]. Examples for electrons include the use of plasmas to process materials and to sterilize medical products. In the case of positrons, one important application is the use of buffer gases to slow high-energy positrons and to trap and further cool them. Beyond these practical considerations, comparison of electron and positron cross sections is important in understanding the underlying physics of vibrational excitation. In spite of these considerations, only recently has it been possible to make state-resolved measurements of positron-impact vibrational excitation cross sections; and to date, there have been no systematic comparisons of such state-resolved cross sections for electrons and positrons.

One reason for this relative lack of understanding is that sufficiently high-resolution, low-energy positron sources have not been commonly available. The development of cold, trap-based positron beams has made such positron-impact measurements possible [2]. This method is particularly suited to the measurement of absolute, state-resolved integral inelastic cross sections. It has now produced the first such cross sections for both electronic and vibrational excitation of atoms and molecules by positron impact [3,4]. Since integral inelastic electron-impact cross sections are typically not measured directly, this technique also offers the possibility of measuring similar electron-impact cross sections to an accuracy equal or better than that possible using other techniques.

Using this technique, measurements of positron-impact vibrational excitation cross sections for CO, CO_2, H_2, CH_4, and CF_4 have been reported [3,5,6]. A positron-impact measurement of this kind was done previously on the ν_3 mode of CF_4 [3] in an apparatus not specifically designed for such a measurement. Given the importance of CF_4 to obtain rapid cooling of positrons in buffer-gas positron accumulators [4] and to cool positron plasmas in Penning-Malmberg traps when compressed radially with rotating rf electric fields [7], we report here more detailed measurements of this cross section. The CF_4 molecule has four vibrational modes. The only mode observed in our experiments is the ν_3 mode with an excitation energy, $E_{ex}=0.159$ eV. As discussed below, it is plausible that the other three modes were not observed; two others are infrared inactive and the fourth is at a low energy, borderline inaccessible in our experiments.

Study of electron-CF_4 interactions is important in many plasma-assisted material-processing applications as well as in space and atmospheric sciences [8]. We report here direct integral measurements of this electron-impact cross section. There have been previous, systematic comparisons of total and differential elastic cross sections for electrons and positrons [9–12]. There have also been reported positron cross-section measurements for the sum of excitation to the three vibrational modes in CO_2 [12]. The experiments reported here, on the other hand, are capable of sufficiently high-energy resolution to measure state-resolved, integral inelastic cross sections, and as mentioned above, to perform these state-selective measurements for both electrons and positrons in the same apparatus in order to minimize systematic differences.

II. DESCRIPTION OF THE POSITRON SCATTERING EXPERIMENT

The experimental arrangement used to make these measurements has been described in detail previously [4]. It is shown schematically in Fig. 1 and consists of a three-stage buffer gas trap, scattering cell, and retarding potential analyzer. The beam formed by the buffer-gas trap is pulsed, with bursts of 1.5×10^4 positrons (electrons) produced at a 4-Hz rate. Typical energy resolution of the measurements is 25 meV [full width at half maximum (FWHM)]. For positron-impact cross sections, an annihilation plate and NaI detector was used, while electrons were detected using a charge-sensitive diode.

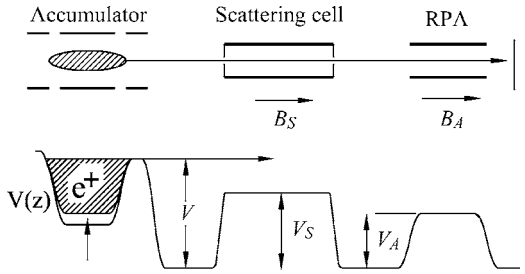

FIG. 1. Schematic diagram of the electrode structure (above) and the electric potentials (below) used to study scattering with a trap-based positron beam. The technique used to measure integral inelastic cross sections relies on the fact that the magnetic fields in the scattering cell and retarding potential analyzer (RPA), B_S and B_A, can be varied independently.

With planned improvements to the current experiment (i.e., a cryogenic, high-field trap potentially capable of providing a beam with 1-meV, FWHM, energy resolution), the resolution of the measurements could approach that of the best electron experiments. If successful, this would further expand the potential uses of the technique.

The vibrational excitation of CF_4 by positron impact, reported in Ref. [3], was done by making minor modifications to an existing three-stage buffer gas trap. Positrons were trapped and cooled in the three-stage trap using an N_2 buffer gas. The N_2 was then pumped out, and CF_4 was introduced into the first stage of the trap, which was used as a scattering cell. Positrons were sent back toward the source through the first trapping stage (i.e., now the scattering cell) and an RPA and then detected.

Following the success of this initial experiment, numerous improvements were made to the experimental apparatus [4]. In the first experiment of Gilbert *et al.* [3], the scattering cell (i.e., the first trapping stage) was 55 cm long and 1.2 cm in diameter. It was differentially pumped on both ends, and the test gas was introduced at the center of the cell. Due to the geometry of the cell and the pumping, the gas pressure dropped by an order of magnitude from the center of the cell to the ends. The current scattering cell, which is located external to the trap (see Fig. 1), is 38.1 cm long and has a relatively large (7.0 cm) inner diameter and small (0.5 cm) apertures at each end. The advantage of the current design is that the gas pressure is essentially constant throughout the entire interaction region, with the drop in pressure occurring in small spatial regions at each end of the cell. Additionally, the design and location of the current cell allows both the trap and the scattering cell to be filled with test gas at all times which allows for a faster repetition rate.

The technique we have developed to measure state-resolved integral cross sections exploits the properties of the positron orbits in a strong magnetic field and the invariance of the ratio $E_\perp/\mathrm{B}$, which is the ratio of the energy in the positron gyromotion about the magnetic field to the magnetic-field strength [3,4]. Good resolution is achieved when the magnetic field in the retarding potential analyzer, B_A, is small compared to the field B_S in the scattering cell. Another improvement in the current experimental setup is an increase in the maximum field ratio, $M=B_S/B_A$, which can be achieved between the scattering region and the analyzing region. This parameter determines the ability to resolve inelastic and elastic scattering and to resolve scattering from different inelastic processes. For the data in Ref. [3], the maximum M value was 3. In the current experiments, $M=35$.

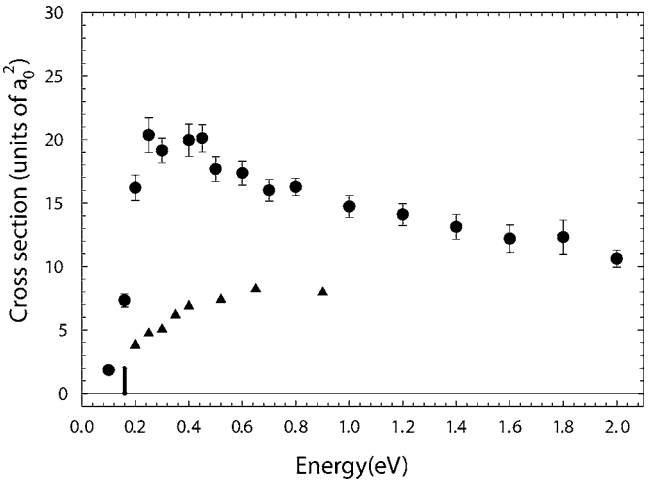

FIG. 2. Present measurements of the integral cross section for the positron-impact vibrational excitation of the ν_3 mode in CF_4 (•). Also shown are the previous results (▲) [3] taken with a different experimental apparatus.

III. POSITRON-IMPACT RESULTS

In Fig. 2, the current data for the vibrational excitation cross section of the ν_3 mode in CF_4 are shown together with the data previously reported in Ref. [3]. The CF_4 molecule has four modes with excitation energies (in eV): ν_1 (0.113), ν_2 (0.054), ν_3 (0.159), and ν_4 (0.078). Only the ν_3 mode was observed. This is likely because the first two modes, ν_1 and ν_2, are infrared inactive, implying that there is no long-range dipole coupling to them; and the ν_4 mode is at the low-energy limit of observability using the current apparatus. The ν_3 mode is also the strongest of the vibrational modes observed in electron scattering [13].

The two positron-impact cross sections shown in Fig. 2 (i.e., the previous and present measurements) are significantly different, both in magnitude and shape. This is perhaps not too surprising considering the improvements to the apparatus and techniques that were made since the first experiment of Gilbert *et al.* [3]. Based upon subsequent experience, it is likely that the close proximity of the scattering cell wall to the positron beam in the first experiment resulted in diffusive losses of positrons to the wall and the trapping of the positrons in the scattering cell, particularly near the threshold of the excitation cross section. This problem was remedied before subsequent state-resolved integral cross-section measurements were made on the other atomic and molecular targets studied to date, namely CO, H_2, CO_2, CH_4, and is detailed in Refs. [5,6].

IV. EXPERIMENTAL MODIFICATIONS FOR ELECTRON-IMPACT MEASUREMENTS

For electrons, the buffer-gas trap is operated in the same way as for the trapping and beam formation of positrons (see

Ref. [4]), but with the voltages reversed. For electrons, the source is the beam of secondary electrons produced at the solid neon moderator [14] by fast positrons from the ^{22}Na positron source. Typical electron fluxes from the moderator result in $\sim 5 \times 10^5$ trapped electrons per second. The detection scheme was modified for the electron experiments. The positron experiments use an annihilation plate, NaI scintillator, and photodiode, with the latter two elements located outside of the vacuum system. For the electron experiments, the detection apparatus was modified to include a charge-sensitive diode located in the vacuum system.

The front surface of the diode was used as the annihilation plate for positron detection. While the diode could be used for positron as well as electron detection, for the data presented here, positrons were detected using the NaI scintillator as described above. Since absolute cross-section measurements are obtained normalizing the inelastic scattering signal to the incident beam, use of different detectors for the electron and positron experiments does not introduce any systematic errors in comparing cross sections for the different projectiles.

In order to do electron experiments with particle fluxes comparable to those used in the positron experiments, it is required that the detector be capable of detecting pulses of 3×10^4 charged particles at a 4-Hz repetition rate with good signal to noise. The detector chosen was a charged particle diode (International Radiation Detectors Inc., model AXUV-576G, http://www.ird-inc.com/). The active surface area of the diode is 2.54×2.54 cm. The diode was biased at $\sim \pm 400$ V, to achieve good detection efficiency for the incoming electrons [15]. A grounded titanium mesh (transmission 81%) mounted on a 316 stainless-steel ring was placed in front of the diode to keep the electric potential on the diode from leaking into the analyzer region of the trap. A separate magnetic field coil in the detector region was used to focus the beam from the low-field region in the RPA onto the active area of the diode.

The diode signal is read out on the anode. A capacitor was placed between the diode and the amplifier to isolate it from the diode bias voltage. A current-to-voltage amplifier circuit was used to amplify the signal, which is proportional to the number of charged particles hitting the diode.

Figure 3 shows the diode responsivity R_M of the charge-sensitive diode as a function of incoming particle energy for both positrons and electrons incident on the diode. This responsivity is defined as

$$R_M = \frac{I_{PD}}{I_0(E_0/e)}, \tag{1}$$

where I_{PD} is the current detected from the diode, I_0 is the incident beam current in amps, E_0 is the energy of the incoming particles in eV, and e is the change of the electron. The intensity of the incident beam, I_0, was measured with a calibrated, charge-sensitive amplifier. Over the range of energies measured (i.e., 100–400 eV), the measured responsivity for both electrons and positrons is in good agreement with that reported in Ref. [15].

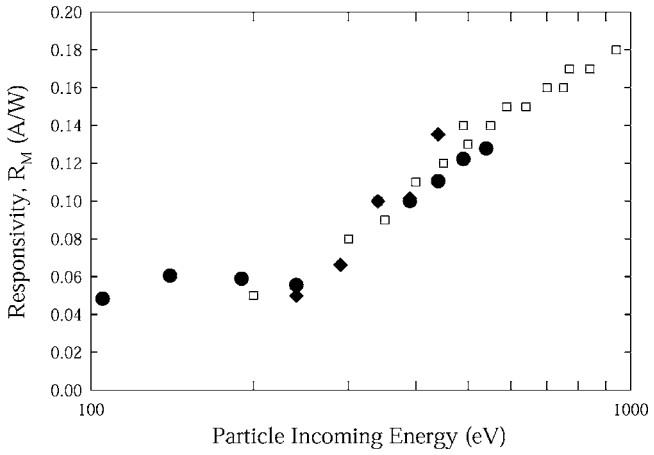

FIG. 3. Responsivity as a function of incoming particle energy. Current data for (•) positrons and (◆) electrons, compared to (□) the responsivity reported in Ref. [15] for incident electrons.

V. VIBRATIONAL CROSS SECTION FOR ELECTRON IMPACT

As mentioned above, one area in which this apparatus can make significant contributions is measurement of low-energy, state-resolved integral inelastic scattering cross sections. This is because the scattering system is already optimized for low-energy investigations, and these types of measurements take advantage of the 25-meV beam resolution and the technique of studying scattering in a strong, spatially varying magnetic field. Additionally, there is a dearth of such integral inelastic cross-section measurements in the literature. As described above, measurements were made of the electron-impact vibrational excitation cross section for the ν_3, asymmetric stretch mode of CF_4, described above (E_{ex}=159 meV). This cross section was measured using the same technique as that used to measure the integral cross section for positron impact [3,4]. The through-beam measurement was taken with the scattering cell and the analyzer grounded.

In Fig. 4 we plot the current results for the integral inelastic, electron-scattering cross-section for the ν_3 mode of CF_4. The error bars are larger than those for the positron data due to excess noise associated with measurements using the charge sensitive detector. Also shown are comparisons with the only other available results for this integral electron-impact cross section. The data from Ref. [16] were estimated from swarm data, renormalized using a correction factor of 0.7 as suggested in Ref. [17]. The data from Ref. [18] were obtained from differential scattering cross-section measurements as a function of angle at several energies and a model (i.e., the Born-dipole approximation, described below) to obtain the integral cross section. To our knowledge, the current data, shown in Fig. 4, *are the only direct integral measurements of this electron-impact cross section*. They indicate a somewhat smaller peak value than that of the other experiments. However, in general, both the absolute values and the shape of the cross section are in reasonably good agreement with the previous measurements.

Also shown in Fig. 4, are the results of an analytic, Born-dipole approximation calculation for the cross section for the mode ν_3, which is given by [13]

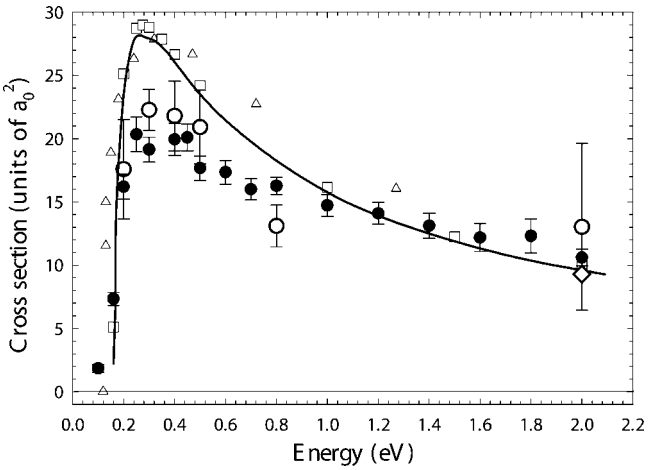

FIG. 4. Integral electron-impact vibrational excitation of the ν_3 vibrational mode of CF_4: (○) current data and (△) results of Ref. [16] scaled by a factor of 0.7 as suggested in Ref. [17]. Shown for comparison (•) are the current positron-impact results. Also shown are (—) the results of an analytic, Born-dipole approximation calculation for the cross section [13], using infrared measurements to fix the dipole strength M_n^d; and (□) [18] the Born model, fixing M_n^d using electron differential scattering cross-section measurements. Shown by the (♦) symbol is the result of a recent local interaction potential calculation for electron impact [19].

$$\sigma = \frac{8\pi}{3k^2} g_n M_n^d \ln[(k+k')/(k-k')], \tag{2}$$

where all quantities are in atomic units, k and k' are the initial and final positron (electron) momenta, g_n is the mode degeneracy, and M_n^d is the square of the dipole matrix element. For the ν_3 mode of CF_4, $g_n=3$, and the transition dipole strength $g_n M_n^d = 0.045$, as determined by infrared absorption measurements [13,20]. The agreement of both the magnitude and shape of the cross section predicted by the Born model with the current data is reasonably good, including the sharp rise at onset.

The fact that the Born dipole model yields good quantitative agreement with the data explains in a natural way the similarity of the electron and positron cross sections. Namely, for this molecule, the long-range electrostatic coupling (i.e., expected to be identical for positron and electron impact) is the dominant coupling to this ν_3 asymmetric stretch mode. This strong coupling likely arises from the large amount of charge transfer from the carbon to the fluorine atoms.

The local-interaction potential calculation of Irrera and Gianturco [19] for electron excitation of CF_4 was done from 2 eV upward, so the only point of overlap with the present measurements is at this one energy of 2 eV. As shown in Fig. 4, the prediction of this calculation is in good agreement with both the data and the Born dipole model at this energy. However, the slope of the theoretically predicted cross section, $d\sigma/dE$, where E is the incident positron energy, is positive at this point, whereas slopes given by the Born model and the data are zero or slightly negative at this energy.

The strong similarity of positron- and electron-impact cross sections seen here is not always the case. For example, the positron- and electron-impact vibrational cross sections for excitation of the ν_1 mode in CO have very different shapes and magnitudes. The electron cross section for CO has a peak value about ten times larger than, and peaks about 1.5 eV above, the peak in the positron cross section, due to an electron shape resonance in CO [1]. To date, no such shape resonances have been identified in positron-impact vibrational cross sections.

Future experiments will benefit from additional improvements to the current apparatus. The grounded mesh in front of the detector is a potential source of secondary electrons. It could be replaced by an arrangement of cylindrical electrodes, which would eliminate this extrinsic effect. In addition, in the electron experiments, a significant population of low-energy electrons was observed coming from the trap when the electron beam was formed. This low-energy component could be reduced by better differential pumping between the trap and the scattering cell, and/or by the introduction of an additional electrode, used as a high-pass filter, between the electron trap and the scattering cell.

A major adaptation of the experimental apparatus for electrons was use of a detector (based on charge collection instead of positron annihilation) that has adequate signal to noise to measure bursts of $\sim 10^4$ electrons at a 4-Hz rate. The detector used here appears to be adequate for this purpose, but may well not be the ultimate best choice.

VI. FURTHER COMPARISONS WITH THE BORN DIPOLE MODEL

As shown in Fig. 4, there is good agreement between the predictions of the Born dipole model and the positron and electron impact results for CF_4. Given this agreement, it is of interest to make similar comparisons for the other molecules for which state-resolved, positron-impact vibrational cross sections have been measured, namely H_2 (infrared inactive), CO, CO_2, and CH_4 [5,6]. While the situation can indeed be more complicated when more than one vibrational excitation mechanism is operative, comparison with the Born dipole model can be regarded as an estimate of the degree to which long-range dipole coupling explains the observed cross sections.

For the targets studied thus far that have nonzero transition dipole moments, the *shapes* of the Born-dipole cross sections are in fair agreement with the measurements. For example, shown in Fig. 5 is a comparison of the Born model with data for the ν_3 mode of CO_2 [5]. In this case, the Born dipole prediction accounts for about 60% of the measured value and has a shape virtually identical to that measured. The comparison of the magnitude of the measured cross section with the Born model prediction varies widely among the molecules studied to date, from essentially all of the cross section for the ν_3 mode in CF_4 to about 30% of the cross section for the unresolved $\nu_2+\nu_4$ modes in CH_4 (where only the ν_4 mode is IR active) and about 20% of the cross section for the unresolved $\nu_1+\nu_3$ modes in the same target (only the ν_3 mode is IR active). In H_2, the Born dipole model predicts a null cross section due to symmetry. Further details of the comparison of the Born dipole model with the positron-

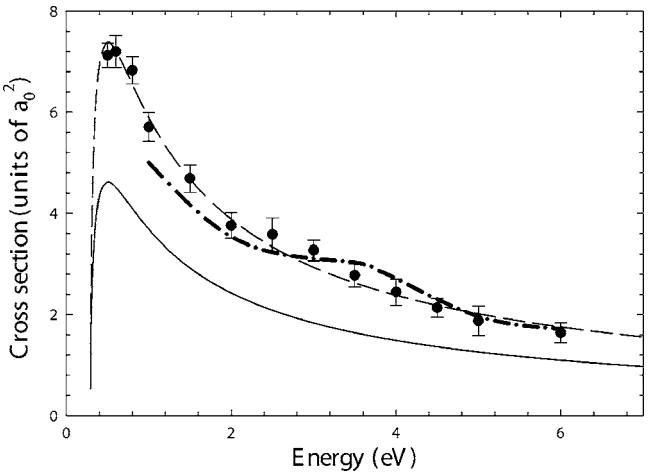

FIG. 5. Comparison of (•) the integral positron-impact cross section for vibrational excitation of the ν_3 mode of CO_2 [5] with the predictions of the Born dipole model. Shown are (—) the results of an analytic, Born-dipole calculation, (– –) the Born-dipole calculation scaled by a factor of 1.6, and (– · –) a calculation for positron-impact using a close coupling and continuum multiple scattering approach [12]. This comparison indicates that the predictions of the long-range dipole-coupling model can account for both the shape and much of the magnitude of the observed cross section.

impact vibrational excitation cross sections for which data is available will be discussed elsewhere [21].

VII. CONCLUDING REMARKS

We present here improved measurements of the integral positron-impact cross section for excitation of the ν_3 vibrational mode in CF_4. The resulting cross section for CF_4 is comparatively large (i.e., at its peak $\sim 20a_0^2$), the largest positron-impact vibrational cross section measured to date by more than a factor of 2. This large inelastic scattering cross section in CF_4 and its comparatively small positron annihilation cross section [22] explains why CF_4 is the molecule of choice for cooling in buffer-gas positron traps and other positron plasma experiments [4,7].

Another interesting feature of the CF_4 data reported here is the quantitative similarity of the electron and positron cross sections. This is in contrast to essentially all other molecules for which both electron and positron vibrational excitation data are available. Typically neither the magnitude nor the shapes of the cross sections are as similar as they are in CF_4. Both the large magnitude and the similarity of the electron and positron cross sections agree well with the predictions of the Born dipole model and are likely due to the large amount of charge transfer from carbon to the fluorines in this molecule. Comparison of the positron-impact vibrational excitation spectra measured to date indicates varying degrees of agreement with the Born dipole model. A more detailed discussion of this comparison will be presented elsewhere [21].

The work reported here demonstrates the potential of the trap-based beam and associated technique to measure scattering in a strong magnetic field for making systematic comparisons of integral, state-resolved inelastic electron and positron cross sections. The general good agreement between the measurements presented here and other available experimental values for the electron cross section indicates that approach described here is likely to be useful in general in making quantitative, systematic measurements of integral inelastic positron- and electron-impact cross sections.

ACKNOWLEDGMENTS

We thank P. Schmidt for assistance with the diode electron detector, G. Gribakin for suggesting comparison with the Born dipole model and helpful conversations, J. P. Sullivan, S. J. Buckman, and J. Danielson for helpful conversations, and E. A. Jerzewski for his expert technical assistance. This work was supported by the National Science Foundation, Grant No. PHY 02-44653.

[1] C. M. Surko, G. F. Gribakin, and S. J. Buckman, J. Phys. B **38**, R57 (2005).
[2] S. J. Gilbert, C. Kurz, R. G. Greaves, and C. M. Surko, Appl. Phys. Lett. **70**, 1944 (1997).
[3] S. J. Gilbert, R. G. Greaves, and C. M. Surko, Phys. Rev. Lett. **82**, 5032 (1999).
[4] J. P. Sullivan, S. J. Gilbert, J. P. Marler, R. G. Greaves, S. J. Buckman, and C. M. Surko, Phys. Rev. A **66**, 042708 (2002).
[5] J. P. Sullivan, S. J. Gilbert, and C. M. Surko, Phys. Rev. Lett. **86**, 1494 (2001).
[6] J. P. Sullivan, S. J. Gilbert, J. P. Marler, L. D. Barnes, S. J. Buckman, and C. Surko, Nucl. Instrum. Methods Phys. Res. B **192**, 3 (2002).
[7] R. G. Greaves and C. M. Surko, Phys. Rev. Lett. **85**, 1883 (2000).
[8] L. G. Christophorou, J. K. Olthoff, and M. V. V. S. Rao, J. Phys. Chem. Ref. Data **25**, 1341 (1996).
[9] E. Surdutovich, W. E. Kauppila, C. K. Kwan, E. G. Miller, S. P. Prikh, K. A. Price, and T. S. Stein, Nucl. Instrum. Methods Phys. Res. B **221**, 97 (2004).
[10] S. Zhou, H. Li, W. E. Kauppila, C. K. Kwan, and T. S. Stein, Phys. Rev. A **55**, 361 (1997).
[11] C. Makochekanwa, M. Kimura, and O. Sueoka, Phys. Rev. A **70**, 022702 (2004).
[12] M. Kimura, M. Takekawa, Y. Itikawa, H. Takaki, and O. Sueoka, Phys. Rev. Lett. **80**, 3936 (1998).
[13] A. Mann and F. Linder, J. Phys. B **25**, 545 (1992).
[14] R. G. Greaves and C. M. Surko, Can. J. Phys. **51**, 445 (1996).
[15] H. O. Funsten, D. M. Suszcynsky, S. M. Ritzau, and R. Korde, IEEE Trans. Nucl. Sci. **44**, 2561 (1997).
[16] M. Hayashi, in *Swarm Studies and Inelastic Electron-Molecule Collisions*, edited by L. C. P. *et al.* (Springer, Berlin, 1987), pp. 167–187.
[17] L. E. Kline and T. V. Congedo, Bull. Am. Phys. Soc. **34**, 325

(1989).
[18] R. A. Bonham, Jpn. J. Appl. Phys., Part 1 **33**, 4157 (1994).
[19] S. Irrera and F. A. Ginaturco, New J. Phys. **7**, 1 (2005).
[20] L. M. Bishop and L. M. Cheung, J. Phys. Chem. Ref. Data **11**, 119 (1982).
[21] J. P. Marler and C. M. Surko, Nucl. Instrum. Methods Phys. Res. B (to be published).
[22] K. Iwata, R. G. Greaves, T. J. Murphy, M. D. Tinkle, and C. M. Surko, Phys. Rev. A **51**, 473 (1995).